

SIXTH INTERNATIONAL WORKSHOP on TROPICAL CYCLONES

Topic 1.4 : Operational Techniques in Defining TC Structure

Rapporteur: Mark A. Lander
University of Guam
UOG Station
Mangilao, Guam (USA) 96923

Email: mlander@uog.edu

Fax: 1-671-734-8890

Working Group: A. Zhao, C.-S. Liou, K. Cheung, R. Edson, and J. Franklin

Abstract:

Tropical cyclone warnings to the public typically include forecasts of the weather elements that contribute to hazards that may threaten lives or cause substantial damage to infrastructure, homes, crops and other physical assets. Traditionally, the TC warning issued to the public contains information on the expected wind speeds, rainfall amounts, and sea inundation. There is often a broad-brush statement on the level of damage to be expected. TC structures that are important to the operational forecast and warning efforts include:

- (1) surface wind distribution;
- (2) eye characteristics;
- (3) vertical structure of the wind and temperature;
- (4) Satellite-observed cloud patterns;
- (5) critical boundary layer profiles (e.g., changes as TC moves over colder water)
- (6) sub-kilometer scale wind patterns in the TC core that might have a substantial impact on air-sea exchanges.

Even at the most sophisticated of operational centers, one might consider the techniques for determining TC structure (e.g., wind distribution and intensity estimation) fairly primitive. The techniques for estimating TC intensity from satellite imagery have changed little in 30 years. There is, however, a vast array of new sensors and applications that should greatly improve the ability of forecasters to diagnose the TC structures that are critical to the making of accurate forecasts and improved public warnings.

This report highlights some of the key technologies that promise great advances in operational ability to diagnose TC structure. The TC community must convey to policy makers the high priority of these technologies. There are many sensors that help the forecaster to diagnose TC structure. The conventional visible and infrared satellite pictures are the "bread and butter" of TC structure diagnosis, and will continue to be the anchor sensors for determining TC structure.

1.4.1: Overview

The primary characteristic of a tropical cyclone that is used to assess and anticipate the threat to human life and property is the intensity, which is normally given as the maximum wind speed in the TC core. The Saffir-Simpson Hurricane Damage Potential Scale is one of the few resources available to relate a forecast wind speed in a TC to expected levels of damage. The minimum sea level pressure in the TC center is also used as a measure of intensity. Lowered surface pressure in the TC core,

however, is not a primary hazard, but does contribute to coastal inundation through the inverse barometric rise of sea level.

Other structural characteristics of a TC that have operational importance in the preparation of forecasts and warnings include:

- (1) the surface wind distribution;
- (2) the eye characteristics (e.g., concentric or annular);
- (3) the vertical structure of the wind and temperature; and,
- (4) the spatial extent and organization of deep convection;

Small-scale wind transients such as TC-associated tornadoes are also important structural features of TCs. Other small-scale characteristics of a TC may have important implications for local wind conditions; for example, the boundary layer temperature profile and changes to this profile such as those occurring when a TC moves over colder water. Some esoteric characteristics of the TC core such as the sub-kilometer scale wind depiction provided by high-resolution Doppler radar may prove to be beneficial for numerical forecasts of high-impact TC structures, such as the intensity.

1.4.2. The TC surface wind distribution

For many years, conventional visible (VIS) and infrared (IR) satellite imagery has provided the input data for the diagnosis of TC intensity and wind distribution. Dvorak's techniques (developed in the early 1970s) became operational with the introduction of his techniques for estimating TC intensity from visible satellite imagery (Dvorak 1975), and the techniques for estimating TC intensity from enhanced infrared satellite imagery (Dvorak 1984). Aircraft reconnaissance of TCs is routinely available only in the Atlantic basin. Many of the operationally important structural characteristics of TCs can be obtained from the aircraft platform; otherwise, meteorological satellites, synoptic observations and ground-based radar (where available) must be used to determine TC structure.

The diagnosis of TC surface wind distribution has not seen substantial improvement until recent advances occurred in remote-sensing technologies, including active microwave sensors on satellites and aircraft. Historical efforts to diagnose TC wind distribution have primarily rested on determination of the size of the TC from conventional satellite imagery. The outer wind distribution is then obtained using an analytical TC wind profile (e.g., Holland 1980) anchored by the estimated size and intensity. There are typically five bins of TC size (very small, small, average, large, and giant) of Brand (1972) and Merrill (1982). At the Joint Typhoon Warning Center (JTWC) Guam (in Hawaii after 1998), the values in Table 1 were used – in the absence of other evidence to the contrary – to assign wind radii to TCs. This table was used at the JTWC at least through the mid 1990s (Edson, personal communication). Of course, any other reliable data depicting the actual wind radii of a given TC trumped the values obtained in Table 1 – especially wind vectors obtained by scatterometer. Other considerations used to fine-tune the diagnosis and forecasts of TC wind distribution included: the TC movement; the synoptic environment; the diameter of the eye (especially as revealed by passive microwave imagery); land effects; and extratropical transition.

Powell et al. (1998) developed a technique (the "H*wind" software) to derive the surface wind speeds in a TC. H*Wind is an analysis package that, like any other analysis scheme, takes observations at specific locations (like along aircraft legs) and deduces a complete surface wind-field depiction for the entire domain of the TC. Forecasters at the NHC weren't completely satisfied with the accuracy and consistency of the technique. Some contentious issues included the appropriateness of presenting to the public a depiction of the surface winds in the entire TC when the wind field was sampled only in limited areas; and the propriety of adjusting flight-level winds downward to deduce a surface wind distribution over the entire cyclone. For reasons such as these, it was not implemented operationally (Franklin, personal communication).

At the NHC, one might consider the techniques for determining the wind distribution fairly primitive. Traditionally the flight-level winds are printed out in hard copy format, and dividers are used on these

plots to estimate the operational wind radii (64, 50, 34 kt radii in the 4 quadrants). When this is done, a standard set of surface wind adjustment factors derived from dropsonde data are used. Very recently, the NHC gained the technical capacity to locally ingest the flight-level winds into N-AWIPS, thus one can display the recon winds along with all the other observations (ships, buoys, METARs, QuikSCAT, etc.) on one screen with the satellite imagery. There are distance tools in N-AWIPS, so it is likely that this is how operational wind radii will be obtained until further advances are forthcoming. N-AWIPS can also adjust the flight-level wind speeds using the dropsonde adjustment factors. Just recently (early September 2006) SFMR ingest was implemented. The NHC is moving rapidly toward a single display platform for all of these data.

The use of airborne radar to depict structure operationally is in its infancy. There is a Joint Hurricane Testbed (JHT) project ongoing in the U.S. to develop displays of vertical and horizontal reflectivity and Doppler velocity data that could be used by the forecaster to assess some important TC structural characteristics (e.g., banding, concentric eyewall, wind distribution, etc.) None of this has quite made it into operations yet -- maybe within a year or two.

1.4.3 Eye Characteristics

One of the most important structural features of a TC is the character of the eye. Operational techniques for determining TC intensity, TC wind distribution, and other metrics (such as the radius of maximum wind) depend on accurate knowledge of the eye structure. Dvorak's techniques for determining TC intensity from satellite imagery are heavily dependent on the structure of the eye. Advances in remote sensing -- in particular, microwave imagers -- now enable forecasters to see details of eye structure through dense cirrus. The implications of the properties of the TC eye as seen on microwave imagery are only now beginning to be understood.

Two features of eye structure have received recent operational attention: (1) Eyewall replacement cycles (Willoughby et al. 1982 and Willoughby 1990), and (2) annular hurricanes (Knaff et al. 2003).

(a) Concentric eyewalls

"Concentric eyewall cycles" (or "eyewall replacement cycles") naturally occur in intense tropical cyclones, i.e. major hurricanes (winds > 50 m/s, 100 kt, 115 mph) or Categories 3, 4, and 5 on the Saffir-Simpson scale. During the replacement phase, the tropical cyclone typically weakens. Eventually the outer eyewall replaces the inner one completely and the storm can be the same intensity as it was previously or, in some cases, even stronger. A TC may undergo more than one concentric eyewall cycle. For example, Hurricane Allen (1980) went through repeated eyewall replacement cycles -- going from Category 5 to Category 3 status several times. Microwave imagery greatly enhances the ability of the forecaster to ascertain concentric eyewalls and ongoing replacement cycles.

(b) Annular Hurricanes

An annular hurricane is a tropical cyclone that features a large, symmetric eye (Fig. 1) surrounded by a thick ring of intense convection. This type of TC is not prone to the fluctuations in intensity associated with eyewall replacement cycles, unlike typical intense TCs. Forecasters have difficulty predicting the behavior of annular hurricanes; they are a relatively recently recognized phenomenon. Annular hurricanes are axisymmetric -- symmetric along every radial axis, i.e. very circular in appearance. They lack the spiralform rainbands that are characteristic of typical TCs. After reaching peak intensity, they weaken much more slowly than non-annular storms of similar intensity. However, most annular hurricanes have annular characteristics for only a portion of their lifetimes. Annular hurricanes maintain their intensities longer than usual after their peaks. Statistics show that forecasters significantly overestimate the lessening of wind velocities in annular hurricanes. In terms of the Dvorak technique, annular hurricanes weaken very slowly after their peak (on average, less than 0.5 T after one day from their peak intensities). Research into the characteristics and formation of annular hurricanes is still in its infancy. First classified and categorized in 2002, little is known about how they form, or why some are able to maintain their intensity in hostile conditions. What meteorologists do know is that a normal hurricane, after undergoing an eyewall replacement cycle, fails to re-establish the

standard hurricane appearance. The new eyewall thickens, and rainbands dissipate, and the hurricane takes on an annular structure. As compared to the formation of normal hurricanes, this happens under weaker wind shear and, surprisingly, cooler sea surface temperatures.

1.4.4 Vertical Structure of the wind and temperature

One of the most vexing operational decisions is whether or not to issue TC advisories on cyclones that may not possess all of the characteristics that are normally thought to define a TC. The so-called subtropical cyclone is a prime example. Monsoon depressions in the western Pacific and in the Indian Ocean also fall into this problematic category of cyclones that do not possess the features common to "normal" TCs. Beginning in 2002, the U.S. National Hurricane Center began to number and name subtropical cyclones. In addition, the numbering and naming of the subtropical cyclones follow the natural sequence of the numbering and naming system for the tropical cyclones. Hebert and Potat (1975) provided a description of the characteristics of the subtropical cyclone that still applies today. The subtropical cyclone typically has only a weak lower tropospheric warm-core structure resulting from the lack of sustained convection near the cyclone center. A large radius of maximum winds is associated with these cyclones. To obtain the satellite classification of a subtropical cyclone is a simple process of looking at a series of satellite pictures of subtropical cyclones of various intensities and choosing the one that best applies to the case in question. The NHC strategy has worked well, and all of the named subtropical cyclones since 2002 have made the transition to tropical (though this need not be the case).

Recent work by Hart (2002) gives a quantitative way to track a cyclone through a 3-D phase space based on the thermal wind in the core of the cyclone in the lower-troposphere, the thermal wind in the core of the cyclone in the upper troposphere, and the horizontal temperature gradient in a section drawn across the core of the cyclone. The previously sharp boundary distinguishing tropical cyclones from extratropical cyclones in the first half of the 20th century has been substantially weakened.

Techniques for recovering the vertical temperature profile and the sea level pressure in tropical and subtropical cyclones from satellite-observed microwave emission has helped the forecaster to assess the nature of a particular cyclone. The Advanced Microwave Sounding Unit (AMSU) provides operationally useful information about TC structure. The Microwave Sounding Unit (MSU) began service in 1978 on TIROS-N and continued on the NOAA 6 through 14 satellites. AMSU flies on the NOAA KLM and N satellites as well as NASA's Aqua.

There is strong relationship between the brightness temperature anomalies as measured by the AMSU-A instrument and TC intensity (<http://amsu.ssec.wisc.edu/explanation.html>). The CIMSS AMSU algorithm uses this relationship to estimate TC MSLP. In general during the early stages of TC development the associated warm core is located near channel 7 and that channel is used to produce an estimate. As the TC intensifies the warm core moves higher in the atmosphere closer to the mean location of channel 8. Experience indicates that once the TC reaches hurricane intensity channel 8 tends to be the better indicator of storm strength and the algorithm uses that channel.

1.4.5 Summary of new instrumentation for observing TC structure

Microwave sensors offer a chance to greatly improve the diagnosis of TC structure. These sensors are both active (e.g., QuikSCAT, the TRMM precipitation radar, and the stepped-frequency microwave radiometer used on hurricane reconnaissance aircraft) and passive (e.g., the TRMM microwave imager and the microwave imagers onboard many polar-orbiting satellites). These technologies provide data that should greatly improve the ability of forecasters to diagnose the TC structures that are critical to the making of accurate forecasts and improved public warnings.

(a) QuikSCAT

The QuikSCAT satellite is a polar-orbiting, sun-synchronous satellite with an equator-ascending time of approximately 0600 local (+/- 30 minutes). Wind vector solutions and up to four ambiguity solutions are stored in 25 km X 25 km wind vector cells over an 1800 km wide swath. Besides including the position of the center of each cell, each cell also contains various flagging indicators that include possible contamination with rain, land, and ice. Combining the QuikSCAT data with that of other recent satellite-based remote sensing data can provide a clear and very accurate analysis of TC position and outer wind radii from the genesis phase all the way through to the extratropical transition phase of development, and finally provide a 'minimum' (at least) maximum intensity for those systems just at or below hurricane intensity. In a special case, the high resolution NRCS image can reveal the structure of the TC during an eyewall replacement cycle.

Forecasters were initially reluctant to use the Quikscat ocean surface wind products (e.g., <http://manati.orbit.nesdis.noaa.gov/quikscat/> and http://www.nrlmry.navy.mil/sat-bin/scatt_winds.cgi) to diagnose TC surface wind structure because of the perception that some of the problems in the wind retrievals (e.g., effects of rain and wind directional ambiguities) rendered the product unfit, or too difficult to interpret. However, relentless efforts by Edson (e.g., Edson 2002, Edson and Chang 2003, and Edson and Lander 2003) and others (Liou and Jin 2006) revealed that the QuikSCAT wind retrievals and the raw data stream from the satellite (i.e., the normalized radar cross section – NRCS) could readily be interpreted to yield invaluable information about TC structure.

(b) The Stepped-Frequency Microwave Radiometer (SFMR)

Measurement of the hurricane surface wind field, and in particular the estimation of wind maxima, has long been a requirement of the Tropical Prediction Center/National Hurricane Center (TPC/NHC). The NOAA/Hurricane Research Division's (HRD) Stepped-Frequency Microwave Radiometer (SFMR), built by ProSensing Inc., is the prototype for a new generation of airborne remote sensing instruments designed for operational surface wind estimation in hurricanes. The first experimental SFMR surface wind measurements were made in Hurricane Allen in 1980, the first real-time retrieval of winds on board the aircraft in Hurricane Earl in 1985, and the first operational transmission of winds to TPC/NHC in Hurricane Dennis in 1999. Uhlhorn and Black (2003) determined that surface winds measured by the SFMR are comparable to the Global Positioning Systems (GPS) dropwindsonde measurements that are the current standard. GPS dropwindsondes are instrument packages designed to measure wind speed, temperature and humidity as they drop from the aircraft to the surface. The benefit of the SFMR is that winds are continuously measured during research flights, allowing for more complete mapping of hurricane surface wind structure.

The active 2005 hurricane season in the Atlantic offered several opportunities to test the SFMR algorithm under extreme wind conditions. Details of The Extreme Wind SFMR Algorithm Adjustment, 2005 are found at <http://www.aoml.noaa.gov/hrd/project2005/katrinasfmr.html>. NOAA WP-3D flights into Hurricanes Katrina and Rita provided the first opportunity to confirm the ability of the pod-mounted production version of the SFMR to measure extreme surface wind speeds, i.e. surface wind speeds in excess of 120 kt. It appears that over the entire range of hurricane force winds (i.e. > 64 kt), the emissivity/windspeed relationship may in fact be linear, as opposed to the quadratic behavior previously employed. One can see that the effect of the new fit is to remove the observed small (< 5kt) high bias in the mid range of wind speeds, i.e. 50-100 kt. At the same time the high-wind linear fit also corrects the low bias at extreme winds, i.e. > 115 kt, that had been interpreted incorrectly as a high wind 'roll-off'. Further, it can be concluded that the slight high wind bias in the mid-range was due to the erroneous choice of a quadratic algorithm extending to high winds.

(c) The TRMM precipitation radar

The active radar aboard the TRMM satellite, the TRMM precipitation radar (TRMM-PR), has proven useful in the diagnosis of TC structure. Kodama and Yamada (2005) examined the eye detectability and configuration of 138 TC cases in the western North Pacific during 1998-2002 using satellite

infrared (IR) imageries and the TRMM-PR. It was found that TC eyes were detectable in PR data in 89% of cases and in IR data in only 37% of cases. The cases when the eye was detected both in IR and PR data are mostly the TCs with stronger intensity. In most cases, eye diameter was smaller in IR observations than in PR observations because an upper cloud shield extending from the eyewall partially covered the eye. Cecil et al. (2002) examined 261 TRMM satellite overpasses of 45 hurricanes during 1997-1998. The study focused on the distribution of radar reflectivity values, passive microwave ice scattering magnitudes, and total lightning among the eyewall, inner rainband and outer rainband. It was found that for nearly half of the hurricane's raining area, measurable radar echo (≥ 17 dB) does not extend more than 2 km above freezing level. The median echo top extends to 8 km in the convective rainbands and up to 9 km in the eyewall. Most of the rain areas are stratiform with only 9% of the eyewall region meets the "convective certain" criteria. In addition, lightning flash densities are four times greater in the eyewall region and outer rainband region than in the inner rainband region, which is partially attributed to the stratiform nature of the inner rainband region.

(d) Other sensors

This report highlights QuikSCAT and the SFMR as technologies that promise great advances in operational ability to diagnose TC structure. The TC community must convey to policy makers the high priority of these two technologies. There are many other sensors that help the forecaster to diagnose TC structure: Conventional Visible and Infrared satellite imagery, passive microwave imagery, and ground-based radar. The conventional visible and infrared satellite pictures are the "bread and butter" of TC structure diagnosis, and will continue to be the anchor sensors for determining TC structure.

TC reconnaissance aircraft will likely remain a tool for only the most affluent, but smaller unmanned aerial vehicles (UAVs) may provide a less expensive alternative for *in situ* monitoring of TCs. One such UAV, the Aerosonde (<http://www.aerosonde.com/>) is scheduled in 2006 for single or multiple experiments coordinated with NOAA and AFRES aircraft missions.

Since 2003, the Dropsonde Observations for Typhoon Surveillance near the TAIwan Regions (DOTSTAR; Wu et al. 2005) program has conducted 19 typhoon surveillance missions with the Astra aircraft in North-western Pacific. For some target typhoons, the impact of dropwindsonde data on mesoscale weather prediction was investigated. Experiments were made to test the impact of the subset of the dropwindsonde data, Taiwan terrain, vortex bogusing, and data assimilation schemes.

REFERENCES

- Brand, S., 1972: Very large and very small typhoons of the western North Pacific Ocean. *J. Meteor. Soc. Japan*, 50, 332-341.
- Cecil, D. J., E. J. Zipser, and S. W. Nesbitt, 2002: Reflectivity, ice scattering, and lightning characteristics of hurricane eyewalls and rainbands. Part I: Quantitative description. *Mon. Wea. Rev.*, 130, 769-784.
- Dvorak, V., 1975: Tropical cyclone intensity analysis and forecasting from satellite imagery. *Mon. Wea. Rev.*, 103, 420-430.
- Dvorak, V., 1984: Tropical cyclone intensity analysis using satellite data. NOAA Tech. Report NESDIS 11. Available from NOAA/NESDIS, 5200 Auth Rd., Washington DC, 20233, 47pp.
- Edson, R.T., 2002. Tutorial on QUIKSCAT. Special Focus Topic 1.b. Proceedings of the Fifth WMO International Workshop on Tropical Cyclones (IWTC-V), Cairns, Queensland, Australia. 3-12 December 2002. WMO/TD.

Edson, R.T. and P.S. Chang, 2003 : Normalized radar cross-section patterns from QuikSCAT—A new analysis tool over the tropical ocean. Proc of the 12th Conf on Satellite Meteor. and Oceanography, Long Beach, CA.

Edson, R.T. and M.A. Lander, 2003: A method for integrated satellite reconnaissance fix accuracy. Proceedings of the 12th Conference on Satellite Meteorology and Oceanography, Long Beach, CA.

Hart, R.E., 2003: A cyclone phase space derived from thermal wind and thermal asymmetry. *Mon. Wea. Rev.*, 131, 585–616.

Hebert, P.H., and K.O. Poteat, 1975: A satellite classification technique for subtropical cyclones. NOAA Tech. Memo. NWS SR-83, 25 pp.

Holland G.J., 1980: An analytical model of the wind and pressure profiles in hurricanes. *Mon. Wea. Rev.*, 108, 1212-1218.

Huntley, J.E., 1980: Tropical Cyclone Wind Radius Program. Annual Tropical Cyclone Report of the Joint Typhoon Warning Center, Guam. p 121. NTIS Acquisition Number AD A094668.

Knaff, J.A., J.P. Kossin, and M. DeMaria 2003: Annular Hurricanes. *Weather and Forecasting*, 18, 204-223.

Kodama, Y.-M., and T. Yamada, 2005: Detectability and configuration of tropical cyclone eyes over the western North Pacific in TRMM PR and IR observations. *Mon. Wea. Rev.*, 133, 2213-2226.

Liou C.-S. and Y. Jin, 2004: A Method of Applying QuikSCAT Data for Tropical Cyclone Initialization, Proceedings of the 26th Conference on Hurricanes and Tropical Meteorology, Miami, FL.

Merrill, R.T., 1984: A comparison of large and small tropical cyclones. *Mon. Wea. Rev.*, 112, 1408-1418.

Powell, M. D., S. H. Houston, L. R. Amat, N. Morisseau-Leroy, 1998: The HRD real-time hurricane wind analysis system. *J. Wind Engineer. Ind. Aerody.*, 77&78, 53-64.

Uhlhorn, E.W., and P.G. Black, 2003: Verification of Remotely Sensed Sea Surface Winds in Hurricanes. *Journal of Atmospheric and Oceanic Technology*, 20, 99–116.

Willoughby, H.E., J.A. Clos, and M.G. Shoreibah, 1982: "Concentric eye walls, secondary wind maxima, and the evolution of the hurricane vortex" *J. Atmos. Sci.*, 39, pp.395-411.

Willoughby, H.E. 1990: "Temporal changes of the primary circulation in tropical cyclones" *J. Atmos. Sci.*, 47, pp.242-264

Wu, C.-C., P.-H. Lin, S. Aberson, T.-C. Yeh, W.-P. Huang, K.-H. Chou, J.-S. Hong, G.-C. Lu, C.-T. Fong, K.-C. Hsu, I.-I. Lin, P.-L. Lin, and C.-H. Liu, 2005: Dropwindsonde Observations for Typhoon Surveillance near the Taiwan Region (DOTSTAR): An Overview. *Bull. Amer. Meteor. Soc.*, 86, 787-790.

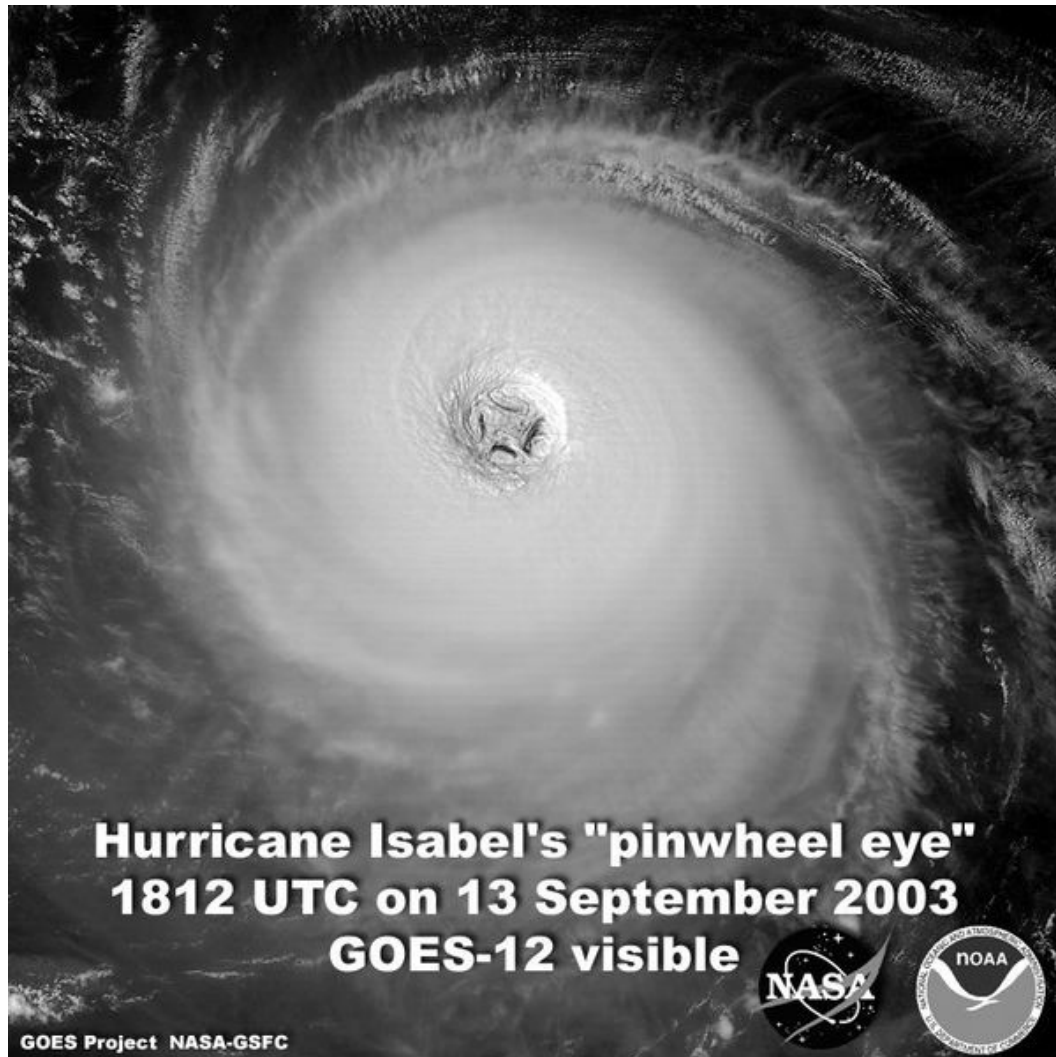


Figure 1. Hurricane Isabel of 2003 showing annular hurricane structure. Notice the large eye (partially filled by eyewall mesovortices) and the relatively few spiral bands around the outside of the storm.

Table 1. Reconstructed wind-radii table used at the JTWC (Sampson and Edson, personal communication)

PREDICTED WIND RADII FOR SPECIFIED WIND INTENSITY (HUNTLEY, 1980, BASED ON TC VORTEX PROFILES BY G. HOLLAND) RADIUS (NM) WIND (KT)																				
VERY SMALL RMW = 10				SMALL RMW = 15				AVERAGE RMW = 20				LARGE RMW = 25				VERY LARGE RMW = 30				INTENSITY
WIND RADII FOR XX KT				WIND RADII FOR XX KT				WIND RADII FOR XX KT				WIND RADII FOR XX KT				WIND RADII FOR XX KT				
100	64	50	34	100	64	50	34	100	64	50	34	100	64	50	34	100	64	50	34	
0	0	0	30	0	0	0	45	0	0	0	60	0	0	0	70	0	0	0	75	35kts
0	0	0	35	0	0	0	55	0	0	0	70	0	0	0	85	0	0	0	95	40kts
0	0	0	40	0	0	0	65	0	0	0	80	0	0	0	100	0	0	0	120	45kts
0	0	15	45	0	0	20	75	0	0	30	90	0	0	35	115	0	0	45	140	50kts
0	0	20	50	0	0	30	85	0	0	40	100	0	0	50	130	0	0	60	160	55kts
0	0	25	60	0	0	40	95	0	0	55	130	0	0	65	155	0	0	80	190	60kts
0	20	30	70	0	35	50	115	0	45	70	150	0	55	85	185	0	65	100	220	65kts
0	20	35	80	0	35	55	125	0	50	80	170	0	60	95	200	0	70	115	245	70kts
0	25	45	90	0	40	65	135	0	55	90	180	0	65	110	220	0	80	130	270	75kts
0	30	50	100	0	40	70	140	0	60	100	195	0	70	120	240	0	85	145	290	80kts
0	30	55	105	0	45	80	155	0	60	105	210	0	75	130	255	0	90	155	310	85kts
0	30	60	110	0	45	85	165	0	65	110	215	0	75	140	270	0	95	165	325	90kts
0	35	65	120	0	50	90	170	0	65	120	225	0	80	150	280	0	100	175	340	95kts
15	35	65	120	15	50	95	175	20	70	125	235	25	85	155	290	35	105	185	355	100kts
15	35	70	125	20	50	100	185	25	70	130	245	30	90	160	300	40	110	195	370	105kt
15	35	70	125	20	50	105	190	30	70	135	250	40	90	165	310	50	110	200	375	110kts
20	40	70	130	25	55	105	190	35	75	140	255	45	95	170	315	55	120	210	390	115kts
20	40	75	135	30	60	110	195	40	80	145	260	50	100	175	320	65	130	215	395	120kts
20	40	75	135	30	65	115	200	45	90	150	265	55	105	180	325	70	135	220	400	125kts
25	45	75	135	35	70	115	205	45	90	150	270	60	110	185	330	75	140	225	410	130kts
25	45	80	140	35	70	120	210	50	95	155	280	65	115	190	335	80	145	230	415	135kts
25	50	80	145	40	75	120	210	55	100	160	285	70	120	195	340	80	145	235	420	140kts
30	50	80	145	40	75	120	215	55	100	160	290	70	125	200	350	85	150	240	425	145kts
30	50	85	150	45	80	125	215	60	105	165	295	75	130	205	355	85	150	245	430	150kts
30	50	85	150	45	80	125	220	65	110	170	300	80	135	210	360	95	160	255	440	160kts
35	55	90	155	50	85	130	225	70	115	175	305	85	140	215	365	100	165	260	450	170kts